

A new spectral method based on two classes of hat functions for solving systems of fractional differential equations and an application to respiratory syncytial virus infection

Somayeh Nemati · Delfim F. M. Torres

Submitted: 26-April-2019; Revised: 02-Nov-2019; Accepted: 17-Dec-2019

Abstract We propose a new spectral method, based on two classes of hat functions, for solving systems of fractional differential equations. The fractional derivative is considered in the Caputo sense. Properties of the basis functions, Caputo derivatives, and Riemann–Liouville fractional integrals, are used to reduce the main problem to a system of nonlinear algebraic equations. By analyzing in detail the resulting system, we show that the method needs few computational efforts. Two test problems are considered to illustrate the efficiency and accuracy of the proposed method. Finally, an application to a recent mathematical model in epidemiology is given, precisely to a system of fractional differential equations modeling the respiratory syncytial virus infection.

Keywords Fractional differential equations (FDEs) · Generalized hat functions · Modified hat functions · Respiratory syncytial virus infection (RSV)

Mathematics Subject Classification (2010) 34A08 · 65M70 · 92D30

S. Nemati
Department of Mathematics,
Faculty of Mathematical Sciences,
University of Mazandaran, Babolsar, Iran
E-mail: s.nemati@umz.ac.ir

Present address: Center for Research and Development in Mathematics and Applications (CIDMA), Department of Mathematics, University of Aveiro, 3810-193 Aveiro, Portugal
E-mail: s.nemati@ua.pt
ORCID: <https://orcid.org/0000-0003-1724-6296>

D. F. M. Torres ✉
Center for Research and Development in Mathematics and Applications (CIDMA), Department of Mathematics, University of Aveiro, 3810-193 Aveiro, Portugal
Tel.: +351-234-370668
Fax: +351-234-370066
E-mail: delfim@ua.pt
ORCID: <https://orcid.org/0000-0001-8641-2505>

1 Introduction

In the last few decades, it has been shown that fractional calculus appears in modeling of many real-world phenomena, in different branches of science where nonlocality plays an essential role, such as physics, chemistry, biology, economics, engineering, signal and image processing, and control theory [Agarwal et al. (2015), Baleanu et al. (2012)], [Malinowska et al. (2015), Morales-Delgado et al. (2019)], [Rekhviashvili et al. (2019), Tariboon et al. (2015)]. This is mainly due to the fact that fractional operators consider the evolution of a system, by taking the global correlation, and not only local characteristics [Almeida et al. (2019)]. As a result, fractional systems have attracted the attention of many researchers in different areas. Nevertheless, obtaining analytic solutions for such problems is very difficult. So, in most cases, the exact solution is not known, and it is necessary to find a numerical approximation. Therefore, many researchers have worked on numerical methods to obtain some numerical solutions of fractional dynamic systems (see, e.g., [Ali et al. (2019), Jafarian et al. (2018), Jafarian et al. (2017), El-Sayed and Agarwal (2019), Nigmatullin and Agarwal (2019)]).

Hat basis functions consist of a set of piecewise continuous functions with shape of hats, when plotted in two dimensional planes. These functions are usually defined on the interval $[0, 1]$ and a generalization of them is obtained by extending the interval into $[0, \tau]$ with any arbitrary positive number τ . Hat basis functions have shown to be a powerful mathematical tool in solving many different kinds of equations. For example, in [Babolian and Mordad (2011)], hat functions have been used to solve linear and nonlinear integral equations of second kind. These functions have been also efficiently employed to solve fractional differential equations (FDEs) [Tripathi et al. (2013)], while in [Heydari et al. (2014)], generalized hat functions are used for solving stochastic Itô–Volterra integral equations. Recently, a modification of hat

functions has been introduced and used in order to solve a variety of problems. To mention some of these problems, we refer to two-dimensional linear Fredholm integral equations [Mirzaee and Hadadiyan (2015)], integral equations of Stratonovich–Volterra [Mirzaee and Hadadiyan (2016a)] and Volterra–Fredholm type [Mirzaee and Hadadiyan (2016b)], and fractional integro-differential [Nemati and Lima (2018)], fractional pantograph nonlinear differential equations [Nemati et al. (2018)] and fractional optimal control problems [Nemati et al. (2019)]. The aim of our work is to have a comparison between these two classes of hat basis functions in solving systems of FDEs.

The paper is organized as follows. Section 2 is devoted to the required preliminaries for presenting our numerical technique. In Section 3, we present the new numerical method, which is based on two classes of hat functions for solving systems of FDEs. Section 4 is concerned with an application of the method for solving a problem in epidemiology related to human respiratory syncytial virus. Finally, concluding remarks are given in Section 5.

2 Preliminaries

In this section, some necessary definitions and properties of fractional calculus are presented. Moreover, two classes of hat functions and some of their properties are recalled.

2.1 Preliminaries of fractional calculus

In this work, we employ fractional differentiation in the sense of Caputo, which is defined via the Riemann–Liouville fractional integral.

Definition 1 [Podlubny (1999)] The (left) Riemann–Liouville fractional integral operator with order $\alpha \geq 0$ of a given function y is defined as

$${}_0I_t^\alpha y(t) = \frac{1}{\Gamma(\alpha)} \int_0^t (t-s)^{\alpha-1} y(s) ds,$$

$${}_0I_t^0 y(t) = y(t),$$

where $\Gamma(\cdot)$ is the Euler gamma function.

Definition 2 [Podlubny (1999)] The (left) Caputo fractional derivative of order $\alpha > 0$ of a function y is defined as

$${}^C D_t^\alpha y(t) = \frac{1}{\Gamma(m-\alpha)} \int_0^t (t-s)^{m-\alpha-1} y^{(m)}(s) ds,$$

where $m-1 < \alpha \leq m$.

For $m-1 < \alpha \leq m$, $m \in \mathbb{N}$, we recall two important properties of the Caputo derivative and Riemann–Liouville integral:

$${}^C D_t^\alpha ({}_0I_t^\alpha y(t)) = y(t),$$

$${}_0I_t^\alpha ({}^C D_t^\alpha y(t)) = y(t) - \sum_{i=0}^{m-1} y^{(i)}(0) \frac{t^i}{i!}, \quad t > 0. \quad (1)$$

2.2 Hat functions

We consider both generalized and modified hat functions.

Generalized hat functions. The interval $[0, \tau]$ is divided into n subintervals $[ih, (i+1)h]$, $i = 0, 1, 2, \dots, n-1$, of equal length h , where $h = \frac{\tau}{n}$. Then, the generalized hat functions (GHFs) are defined as follows [Tripathi et al. (2013)]:

$$\begin{aligned} \psi_0^G(t) &= \begin{cases} \frac{h-t}{h}, & 0 \leq t \leq h, \\ 0, & \text{otherwise,} \end{cases} \\ \psi_i^G(t) &= \begin{cases} \frac{t-(i-1)h}{h}, & (i-1)h \leq t \leq ih, \\ \frac{(i+1)h-t}{h}, & ih \leq t \leq (i+1)h, \\ 0, & \text{otherwise,} \end{cases} \\ \psi_n^G(t) &= \begin{cases} \frac{t-(\tau-h)}{h}, & \tau-h \leq t \leq \tau, \\ 0, & \text{otherwise.} \end{cases} \end{aligned}$$

These functions form a set of $(n+1)$ linearly independent continuous functions in $L^2[0, \tau]$, satisfying the property

$$\psi_i^G(jh) = \begin{cases} 1, & i = j, \\ 0, & i \neq j. \end{cases} \quad (2)$$

An arbitrary function $y \in L^2[0, \tau]$ can be approximated using the GHFs as follows:

$$y(t) \simeq y_n(t) = \sum_{i=0}^n y(ih) \psi_i^G(t) = A^T \Psi_G(t), \quad (3)$$

where

$$\Psi_G(t) = [\psi_0^G(t), \psi_1^G(t), \dots, \psi_n^G(t)]^T \quad (4)$$

and

$$A = [a_0, a_1, \dots, a_n]^T$$

with $a_i = y(ih)$.

Theorem 1 [Tripathi et al. (2013)] If $y \in C^2([0, \tau])$ is approximated by the family of first $(n+1)$ GHFs as (3), then

$$|y(t) - y_n(t)| = O(h^2).$$

Let Ψ_G be the GHFs basis vector given by (4) and $\alpha > 0$. Then,

$$I_t^\alpha \Psi_G(t) \simeq P_G^\alpha \Psi_G(t), \quad (5)$$

where P_G^α is a matrix of dimension $(n+1) \times (n+1)$ called the operational matrix of fractional integration of order α of the GHFs. This matrix is given as [Tripathi et al. (2013)]

$$P_G^\alpha = \frac{h^\alpha}{\Gamma(\alpha+2)} \begin{bmatrix} 0 & \zeta_1 & \zeta_2 & \zeta_3 & \dots & \zeta_n \\ 0 & 1 & \rho_1 & \rho_2 & \dots & \rho_{n-1} \\ 0 & 0 & 1 & \rho_1 & \dots & \rho_{n-2} \\ 0 & 0 & 0 & 1 & \dots & \rho_{n-3} \\ \dots & \dots & \dots & \dots & \dots & \dots \\ 0 & 0 & 0 & 0 & \dots & 1 \end{bmatrix}, \quad (6)$$

where

$$\zeta_i = i^\alpha(\alpha - i + 1) + (i - 1)^{\alpha+1}, \quad i = 1, 2, \dots, n,$$

and

$$\rho_i = (i + 1)^{\alpha+1} - 2i^{\alpha+1} + (i - 1)^{\alpha+1}, \quad i = 1, 2, \dots, n - 1.$$

Modified hat functions. By considering an even integer number n , the interval $[0, \tau]$ is divided into n subintervals $[ih, (i+1)h]$, $i = 0, 1, 2, \dots, n-1$, with equal length $h = \frac{\tau}{n}$. The modified hat functions (MHFs) form a set of $(n+1)$ linearly independent functions in $L^2[0, \tau]$. These functions are defined as follows [Nemati and Lima (2018), Nemati et al. (2018)]:

$$\psi_0^M(t) = \begin{cases} \frac{1}{2h^2}(t-h)(t-2h), & 0 \leq t \leq 2h, \\ 0, & \text{otherwise;} \end{cases}$$

if i is odd and $1 \leq i \leq n-1$, then

$$\psi_i^M(t) = \begin{cases} \frac{-(t-(i-1)h)}{h^2}(t-(i+1)h), & (i-1)h \leq t \leq (i+1)h, \\ 0, & \text{otherwise;} \end{cases}$$

if i is even and $2 \leq i \leq n-2$, then

$$\psi_i^M(t) = \begin{cases} \frac{1}{2h^2}(t-(i-1)h)(t-(i-2)h), & (i-2)h \leq t \leq ih, \\ \frac{1}{2h^2}(t-(i+1)h)(t-(i+2)h), & ih \leq t \leq (i+2)h, \\ 0, & \text{otherwise,} \end{cases}$$

and

$$\psi_n^M(t) = \begin{cases} \frac{1}{2h^2}(t-(\tau-h))(t-(\tau-2h)), & \tau-2h \leq t \leq \tau, \\ 0, & \text{otherwise.} \end{cases}$$

The following property is satisfied for the set of MHFs:

$$\psi_i^M(jh) = \begin{cases} 1, & i = j, \\ 0, & i \neq j. \end{cases} \quad (7)$$

Any function $y \in L^2[0, \tau]$ may be approximated using the MHFs as

$$y(t) \simeq y_n(t) = \sum_{i=0}^n y(ih) \psi_i^M(t) = A^T \Psi_M(t), \quad (8)$$

where

$$\Psi_M(t) = [\psi_0^M(t), \psi_1^M(t), \dots, \psi_n^M(t)]^T \quad (9)$$

and

$$A = [a_0, a_1, \dots, a_n]^T$$

with $a_i = y(ih)$.

Theorem 2 [Nemati and Lima (2018)] *If $y \in C^3([0, \tau])$ is approximated by the family of first $(n+1)$ MHFs as (8), then*

$$|y(t) - y_n(t)| = O(h^3).$$

Let Ψ_M be the MHFs basis vector given by (9) and $\alpha > 0$. Then,

$$I_t^\alpha \Psi_M(t) \simeq P_M^\alpha \Psi_M(t), \quad (10)$$

where P_M^α is a matrix of dimension $(n+1) \times (n+1)$ called the operational matrix of fractional integration of order α of the MHFs. This matrix is given (see [Nemati and Lima (2018), Nemati et al. (2018)]) as

$$P_M^\alpha = \frac{h^\alpha}{2\Gamma(\alpha+3)} \begin{bmatrix} 0 & \beta_1 & \beta_2 & \beta_3 & \beta_4 & \dots & \beta_{n-1} & \beta_n \\ 0 & \eta_0 & \eta_1 & \eta_2 & \eta_3 & \dots & \eta_{n-2} & \eta_{n-1} \\ 0 & \xi_{-1} & \xi_0 & \xi_1 & \xi_2 & \dots & \xi_{n-3} & \xi_{n-2} \\ 0 & 0 & 0 & \eta_0 & \eta_1 & \dots & \eta_{n-4} & \eta_{n-3} \\ 0 & 0 & 0 & \xi_{-1} & \xi_0 & \dots & \xi_{n-5} & \xi_{n-4} \\ \dots & \dots & \dots & \dots & \dots & \dots & \dots & \dots \\ 0 & 0 & 0 & 0 & 0 & \dots & \eta_0 & \eta_1 \\ 0 & 0 & 0 & 0 & 0 & \dots & \xi_{-1} & \xi_0 \end{bmatrix} \quad (11)$$

with

$$\begin{aligned} \beta_1 &= \alpha(3+2\alpha), \\ \beta_i &= i^{\alpha+1}(2i-6-3\alpha) + 2i^\alpha(1+\alpha)(2+\alpha) \\ &\quad - (i-2)^{\alpha+1}(2i-2+\alpha), \quad i = 2, 3, \dots, n, \\ \eta_0 &= 4(1+\alpha), \\ \eta_i &= 4[(i-1)^{\alpha+1}(i+1+\alpha) - (i+1)^{\alpha+1}(i-1-\alpha)], \\ &\quad i = 1, 2, \dots, n-1, \\ \xi_{-1} &= -\alpha, \\ \xi_0 &= 2^{\alpha+1}(2-\alpha), \\ \xi_1 &= 3^{\alpha+1}(4-\alpha) - 6(2+\alpha), \\ \xi_i &= (i+2)^{\alpha+1}(2i+2-\alpha) - 6i^{\alpha+1}(2+\alpha) \\ &\quad - (i-2)^{\alpha+1}(2i-2+\alpha), \quad i = 2, 3, \dots, n-2. \end{aligned}$$

3 Main results

We consider the following general initial value problem, described by a system of m FDEs of order $0 < \alpha \leq 1$:

$$\begin{cases} {}_0^C D_t^\alpha y_1(t) = f_1(t, y_1(t), \dots, y_m(t)), & y_1(0) = y_{1,0} \\ \vdots \\ {}_0^C D_t^\alpha y_m(t) = f_m(t, y_1(t), \dots, y_m(t)), & y_m(0) = y_{m,0}. \end{cases} \quad (12)$$

The aim is to seek functions y_1, \dots, y_m solution of (12) on the interval $0 \leq t \leq \tau$.

3.1 Numerical method

In order to find a numerical solution of (12), we consider approximations of the fractional derivative of the unknown functions as follows:

$${}_0^C D_t^\alpha y_1(t) = A_1^T \Psi(t), \dots, {}_0^C D_t^\alpha y_m(t) = A_m^T \Psi(t), \quad (13)$$

where A_i are the coefficients vectors with the unknown elements $a_{i,j}$, $j = 0, 1, \dots, n$,

$$A_i = [a_{i,0}, a_{i,1}, \dots, a_{i,n}]^T, \quad i = 1, \dots, m, \quad (14)$$

and $\Psi(t)$ equals to either $\Psi_G(t)$, corresponding to the GHFs as the basis functions, or $\Psi_M(t)$, corresponding to the MHFs basis functions. Then, using (1) and the initial conditions given in (12), we can write

$$y_i(t) = A_i^T I_t^\alpha \Psi(t) + y_{i,0}.$$

Using (5) or (10), according to the chosen basis functions, we get

$$y_i(t) = A_i^T P^\alpha \Psi(t) + y_{i,0} = (A_i^T P^\alpha + d_i^T) \Psi(t) = Y_i^T \Psi(t), \quad (15)$$

where

$$d_i = [y_{i,0}, y_{i,0}, \dots, y_{i,0}]^T, \quad Y_i = (A_i^T P^\alpha + d_i^T)^T = [Y_{i,0}, \dots, Y_{i,n}]^T \quad (16)$$

and P^α is given by (6) for the GHFs, or (11) for the MHFs. Therefore, by setting $t = jh$ in (15) and employing (2) or (7), we obtain $y_i(jh) = Y_{i,j}$. Now, we can obtain approximations of the functions $f_i: \mathbb{R}^{m+1} \rightarrow \mathbb{R}$, by using the considered basis functions, as follows:

$$\begin{aligned} f_i(t, y_1(t), \dots, y_m(t)) &= \sum_{j=0}^n f_i(jh, y_1(jh), \dots, y_m(jh)) \Psi_j(t) \\ &= \sum_{j=0}^n f_i(jh, Y_{1,j}, \dots, Y_{m,j}) \Psi_j(t) = F_i(\Theta, Y_1, \dots, Y_m) \Psi(t), \end{aligned} \quad (17)$$

where $\Psi_j(t) = \psi_j^G(t)$ or $\psi_j^M(t)$, and

$$F_i(\Theta, Y_1, \dots, Y_m) = [f_i(0, Y_{1,0}, \dots, Y_{m,0}), f_i(h, Y_{1,1}, \dots, Y_{m,1}), \dots, f_i(\tau, Y_{1,n}, \dots, Y_{m,n})].$$

By substitution (13) and (17) into (12), we have

$$\begin{aligned} A_1^T \Psi(t) &= F_1(\Theta, Y_1, \dots, Y_m) \Psi(t), \\ &\vdots \\ A_m^T \Psi(t) &= F_m(\Theta, Y_1, \dots, Y_m) \Psi(t), \end{aligned}$$

which gives the following system:

$$A_1^T - F_1(\Theta, Y_1, \dots, Y_m) = 0,$$

$$\vdots \\ A_m^T - F_m(\Theta, Y_1, \dots, Y_m) = 0,$$

or

$$a_{i,j} = f_i(jh, Y_{1,j}, \dots, Y_{m,j}), \quad i = 1, \dots, m, \quad j = 0, \dots, n. \quad (18)$$

This system includes $m(n+1)$ nonlinear algebraic equations with $m(n+1)$ unknown parameters, which are the elements of A_i , $i = 1, \dots, m$. By solving this system, approximations of the functions y_i are given by (15).

3.2 Complexity of the resulting systems

The speed of the numerical method given above depends on the speed of solving system (18). Therefore, the form of this system is an important aspect of our method. Here, we display the form of the system given in (18) in detail, for each of the basis functions.

Case 1: GHFs.

According to the form of the operational matrix of fractional integration of the GHFs, given by (6), we can rewrite this matrix as follows:

$$P_G^\alpha = [p_{i,j}^G], \quad i, j = 0, 1, \dots, n,$$

with

$$\begin{aligned} p_{i,0}^G &= 0, & \text{for } i = 0, 1, 2, \dots, n, \\ p_{i,j}^G &= 0, & \text{for } 1 \leq j < i \leq n. \end{aligned}$$

Therefore, the elements of the vectors Y_i , $i = 1, \dots, m$, in (15) are given, using (16), by

$$\begin{aligned} Y_{i,0} &= y_{i,0}, \\ Y_{i,j} &= \sum_{k=0}^j a_{i,k} p_{k,j}^G + y_{i,0}, \quad j = 1, \dots, n. \end{aligned} \quad (19)$$

Taking (19) into account, we rewrite system (18) as follows:

$$a_{i,0} = f_i(0, y_{1,0}, \dots, y_{m,0}), \quad (20a)$$

$$a_{i,1} = f_i\left(h, \sum_{k=0}^1 a_{1,k} p_{k,1}^G + y_{1,0}, \dots, \sum_{k=0}^1 a_{m,k} p_{k,1}^G + y_{m,0}\right), \quad (20b)$$

⋮

$$a_{i,n} = f_i\left(\tau, \sum_{k=0}^n a_{1,k} p_{k,n}^G + y_{1,0}, \dots, \sum_{k=0}^n a_{m,k} p_{k,n}^G + y_{m,0}\right), \quad (20c)$$

$i = 1, \dots, m$. As it can be seen in (20a), the values of the unknown parameters $a_{i,0}$, $i = 1, \dots, m$, are obtained easily by using the initial conditions. By substituting the given $a_{i,0}$ into (20b), we have a system of m nonlinear algebraic equations in unknown parameters $a_{i,1}$, $i = 1, \dots, m$. After solving this system, and substituting the obtained results for $a_{i,1}$ into the m next equations, a system of m equations in $a_{i,2}$, $i = 1, \dots, m$, is obtained. This process continues until $a_{i,n}$, $i = 1, \dots, m$, are found by solving (20c), in which the results for $a_{i,0}, a_{i,1}, \dots, a_{i,n-1}$ have been substituted. Therefore, our method, based on GHFs, reduces the main problem to the solution of n systems of m nonlinear algebraic equations.

Case 2: MHFs.

In a similar way as for GHFs, we rewrite the operational matrix of fractional integration of MHFs as follows:

$$P_M^\alpha = [p_{i,j}^M], \quad i, j = 0, 1, \dots, n,$$

with

$$\begin{aligned} p_{i,0}^M &= 0, & \text{for } i = 0, 1, 2, \dots, n, \\ p_{i,j}^M &= 0, & \text{for } j = 1, 3, \dots, n-1, i = j+2, \dots, n, \\ p_{i,j}^M &= 0, & \text{for } j = 2, 4, \dots, n, i = j+1, \dots, n. \end{aligned} \quad (21)$$

By considering (21) for writing the elements of the vectors Y_i , $i = 1, \dots, m$, in (15), we get

$$\begin{aligned} Y_{i,0} &= y_{i,0}, \\ Y_{i,j} &= \sum_{k=0}^{j+1} a_{i,k} p_{k,j}^M + y_{i,0}, & j = 1, 3, \dots, n-1 \\ Y_{i,j} &= \sum_{k=0}^j a_{i,k} p_{k,j}^M + y_{i,0}, & j = 2, 4, \dots, n. \end{aligned} \quad (22)$$

By substituting the values of $Y_{i,j}$ given in (22) into system (18), this system can be rewritten in detail as follows:

$$a_{i,0} = f_i(0, y_{1,0}, \dots, y_{m,0}), \quad (23a)$$

$$a_{i,1} = f_i\left(h, \sum_{k=0}^2 a_{1,k} p_{k,1}^M + y_{1,0}, \dots, \sum_{k=0}^2 a_{m,k} p_{k,1}^M + y_{m,0}\right), \quad (23b)$$

$$a_{i,2} = f_i\left(2h, \sum_{k=0}^2 a_{1,k} p_{k,2}^M + y_{1,0}, \dots, \sum_{k=0}^2 a_{m,k} p_{k,2}^M + y_{m,0}\right), \quad (23c)$$

⋮

$$a_{i,n-1} = f_i\left(\tau - h, \sum_{k=0}^n a_{1,k} p_{k,n-1}^M + y_{1,0}, \dots, \sum_{k=0}^n a_{m,k} p_{k,n-1}^M + y_{m,0}\right), \quad (23d)$$

$$a_{i,n} = f_i\left(\tau, \sum_{k=0}^n a_{1,k} p_{k,n}^M + y_{1,0}, \dots, \sum_{k=0}^n a_{m,k} p_{k,n}^M + y_{m,0}\right), \quad (23e)$$

$i = 1, \dots, m$. It is seen that the values of the unknown parameters $a_{i,0}$, $i = 1, \dots, m$, are given easily by substituting the initial conditions into (23a). By substituting the given results of $a_{i,0}$ into (23b) and (23c), a system of $2m$ nonlinear algebraic equations in the unknown parameters $a_{i,1}$ and $a_{i,2}$, $i = 1, \dots, m$, is obtained. After solving this system, and substituting the obtained results for $a_{i,1}$ and $a_{i,2}$ into the $2m$ next equations, a system of $2m$ algebraic equations in $a_{i,3}$ and $a_{i,4}$, $i = 1, \dots, m$, is given. By continuation of this process, we find $a_{i,n-1}$ and $a_{i,n}$, $i = 1, \dots, m$, by solving (23d) and (23e), in which the results for $a_{i,0}, a_{i,1}, \dots, a_{i,n-2}$ have been substituted. Our method based on MHFs reduces the system of m nonlinear FDEs to solving $\frac{n}{2}$ systems of $2m$ nonlinear algebraic equations.

3.3 Test problems

In order to illustrate the efficiency and accuracy of the proposed method, we apply it to two test problems whose exact solutions are known.

Example 1 Consider the following system of FDEs:

$$\begin{cases} {}_0^C D_t^{0.5} y_1(t) = \sqrt{t} y_1(t) - y_2(t) + \frac{15\sqrt{\pi}}{16} t^2, & y_1(0) = 0, \\ {}_0^C D_t^{0.5} y_2(t) = \frac{16}{5\sqrt{\pi}} y_1(t) + y_2^2(t) - t^6, & y_2(0) = 0, \end{cases} \quad (24)$$

on the interval $0 \leq t \leq 1$, which has the exact solution

$$y_1(t) = t^{2.5}, \quad y_2(t) = t^3. \quad (25)$$

We have solved this problem by the suggested method, based on GHFs and MHFs, with different values of n , and display

Table 1 Numerical results for problem (24) with different values of n .

n	GHFs					MHFs				
	$y_1(t)$		$y_2(t)$		CPU Time	$y_1(t)$		$y_2(t)$		CPU Time
	$e_{1,n}^G$	$\rho_{1,n}^G$	$e_{2,n}^G$	$\rho_{2,n}^G$		$e_{1,n}^M$	$\rho_{1,n}^M$	$e_{2,n}^M$	$\rho_{2,n}^M$	
2	$1.68e-1$	2.32	$2.24e-1$	1.91	0.000	$2.08e-2$	4.48	$4.57e-2$	3.99	0.000
4	$3.37e-2$	2.13	$5.97e-2$	2.00	0.000	$9.33e-4$	3.45	$2.87e-3$	3.69	0.016
8	$7.68e-3$	2.02	$1.49e-2$	1.99	0.016	$8.51e-5$	3.47	$2.23e-4$	2.86	0.016
16	$1.89e-3$	1.98	$3.74e-3$	1.99	0.031	$7.69e-6$	3.48	$3.08e-5$	2.93	0.047
32	$4.79e-4$	1.98	$9.43e-4$	1.99	0.172	$6.88e-7$	3.49	$4.03e-6$	2.96	0.156
64	$1.21e-4$	1.98	$2.37e-4$	1.99	0.516	$6.12e-8$	3.50	$5.16e-7$	2.98	0.859
128	$3.06e-5$	1.99	$5.97e-5$	2.00	4.453	$5.42e-9$	3.50	$6.53e-8$	2.99	4.609
256	$7.70e-6$	2.00	$1.49e-5$	1.99	23.812	$4.80e-10$	3.50	$8.21e-9$	3.01	23.641
512	$1.93e-6$	—	$3.75e-6$	—	183.688	$4.25e-11$	—	$1.02e-9$	—	196.406

the numerical results in Figure 1, Table 1, and Figure 2. In Figure 1, the approximate solutions of $y_1(t)$ and $y_2(t)$, obtained by employing our method with $n = 2$, are shown. In this figure, the numerical results of $y_1(t)$ and $y_2(t)$, obtained by GHFs, are, respectively, displayed by $y_1^G(t)$ and $y_2^G(t)$. Also, the numerical results of the unknown functions given by MHFs are represented by $y_1^M(t)$ and $y_2^M(t)$. In Table 1, we see the numerical results for the functions $y_1(t)$ and $y_2(t)$, with different values of n , together with the CPU time (in seconds), which have been obtained on a 2.5 GHz Core i7 personal computer with 16 GB of RAM using Mathematica 11.3. For solving the resulting systems of algebraic equations, the Mathematica function FindRoot was used. In this table, the following notations are used for introducing the error and the convergence order of the method:

$$e_{1,n}^G = \max_{0 \leq i \leq n} |y_1(ih) - y_{1,n}^G(ih)|, \quad \rho_{1,n}^G = \log_2 \left(\frac{e_{1,n}^G}{e_{1,2n}^G} \right),$$

$$e_{1,n}^M = \max_{0 \leq i \leq n} |y_1(ih) - y_{1,n}^M(ih)|, \quad \rho_{1,n}^M = \log_2 \left(\frac{e_{1,n}^M}{e_{1,2n}^M} \right),$$

$$e_{2,n}^G = \max_{0 \leq i \leq n} |y_2(ih) - y_{2,n}^G(ih)|, \quad \rho_{2,n}^G = \log_2 \left(\frac{e_{2,n}^G}{e_{2,2n}^G} \right),$$

$$e_{2,n}^M = \max_{0 \leq i \leq n} |y_2(ih) - y_{2,n}^M(ih)|, \quad \rho_{2,n}^M = \log_2 \left(\frac{e_{2,n}^M}{e_{2,2n}^M} \right),$$

where $y_1(t)$ and $y_2(t)$ are the exact solutions, $y_{1,n}^G(t)$ and $y_{2,n}^G(t)$ are the approximate solutions obtained with GHFs, and $y_{1,n}^M(t)$ and $y_{2,n}^M(t)$ are the approximate solutions obtained with MHFs. These results confirm the $O(h^2)$ accuracy order of the numerical method with GHFs and the $O(h^3)$ accuracy order of the numerical method with MHFs. Finally, in Figure 2 (left), the results for the errors obtained by employing our method, for some selected values of n , are plotted in a logarithmic scale. Moreover, the CPU times of the method are plotted in Figure 2 (right). It can be seen that the computational complexity of the resulting systems of GHFs and MHFs are similar.

Example 2 Consider the following system of linear FDEs:

$$\begin{cases} {}_0^C D_t^\alpha y_1(t) = y_1(t) - 2y_2(t) + 4\cos(t) - 2\sin(t), & y_1(0) = 1, \\ {}_0^C D_t^\alpha y_2(t) = 3y_1(t) - 4y_2(t) + 5\cos(t) - 5\sin(t), & y_2(0) = 2, \end{cases} \quad (26)$$

on the interval $0 \leq t \leq 10$. The exact solution of this problem, when $\alpha = 1$, is [Atkinson et al. (2009)]

$$y_1(t) = \cos(t) + \sin(t), \quad y_2(t) = 2\cos(t).$$

We set $\alpha = 1$ and solve the problem. By considering the same notations as introduced in Example 1, we report the numerical results in Table 2. Furthermore, in Figures 3 and 4, the numerical solutions based on GHFs and MHFs, obtained by different values of α and $n = 32$, together with the exact solution with $\alpha = 1$, are plotted. As it could be expected, the numerical solution is close to the exact solution of the corresponding first order problem when α is close to 1.

4 Application to the SEIRS- α epidemic model

We now apply the numerical method introduced in Section 3 to a nonlocal fractional order SEIRS mathematical model, which was recently proposed in [Rosa and Torres (2018)].

4.1 Description of the model

Human respiratory syncytial virus (HRSV) is a virus that causes respiratory tract infections. We refer a reader interested in this virus to [Rosa and Torres (2018)] and references therein. Here we just mention that HRSV is a principal cause of lower respiratory tract infections and hospital visits during infancy and childhood. There is an annual epidemic in temperate climates during the winter season, while in tropical climates this infection is most common throughout the rainy season. Since protective immunity is induced by natural infection with HRSV more than many other respiratory viral infections, people can be infected multiple times even within a single HRSV season.

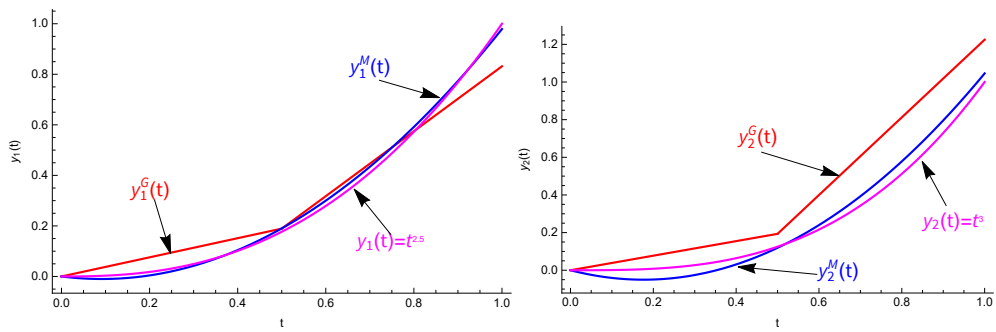


Fig. 1 Numerical results for problem (24) with $n = 2$: results for the function $y_1(t)$ (left); results for the function $y_2(t)$ (right).

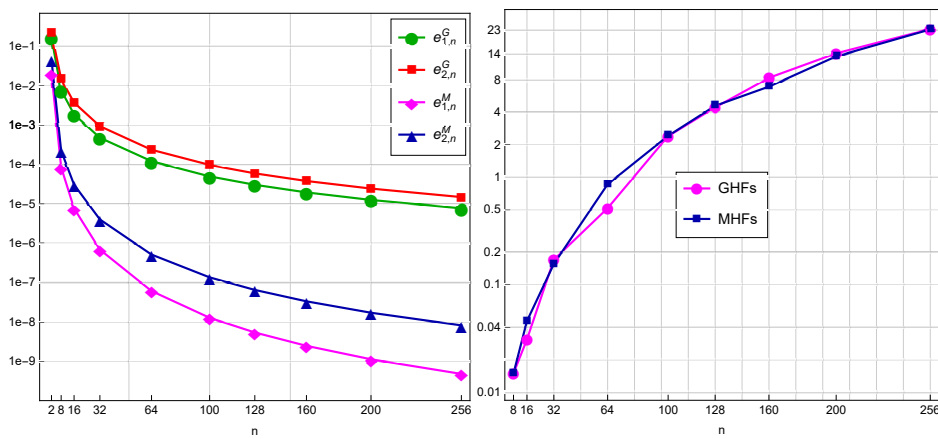


Fig. 2 Errors of the numerical method for solving problem (24) (left); CPU time in seconds (right).

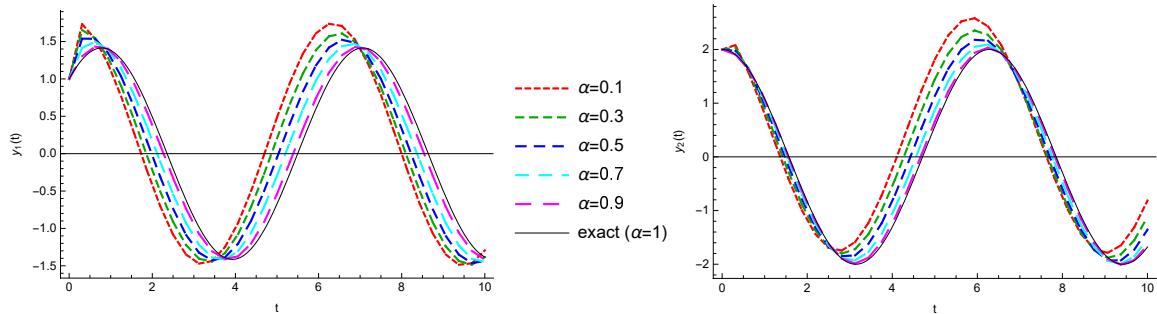


Fig. 3 Numerical results for problem (26) based on GHFs with different values of α and $n = 32$: results for the function $y_1(t)$ (left); results for the function $y_2(t)$ (right).

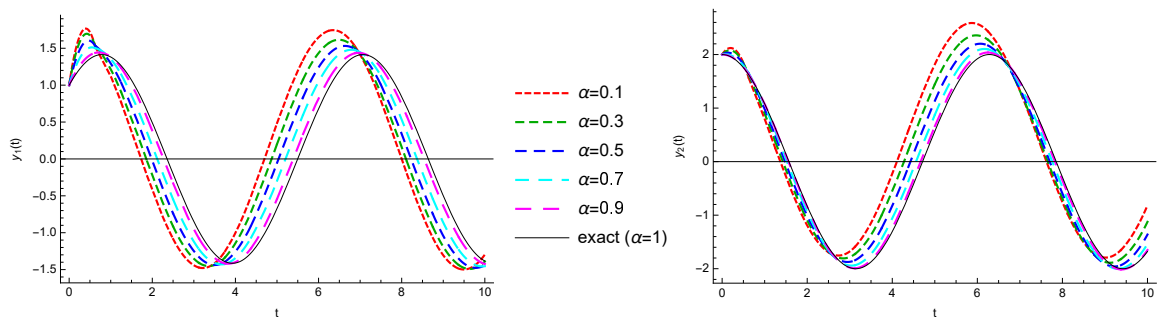


Fig. 4 Numerical results for problem (26) based on MHFs with different values of α and $n = 32$: results for the function $y_1(t)$ (left); results for the function $y_2(t)$ (right).

Table 2 Numerical results for problem (26) with different values of n and $\alpha = 1$.

n	GHFs					MHFs				
	$y_1(t)$		$y_2(t)$		CPU Time	$y_1(t)$		$y_2(t)$		CPU Time
	$e_{1,n}^G$	$\rho_{1,n}^G$	$e_{2,n}^G$	$\rho_{2,n}^G$		$e_{1,n}^M$	$\rho_{1,n}^M$	$e_{2,n}^M$	$\rho_{2,n}^M$	
2	$2.33e+0$	2.22	$2.15e+0$	3.01	0.000	$2.03e+0$	1.26	$1.87e+0$	1.53	0.000
4	$5.01e-1$	1.93	$2.67e-1$	2.31	0.031	$8.47e-1$	3.23	$6.49e-1$	2.48	0.000
8	$1.31e-1$	2.04	$5.38e-2$	1.86	0.031	$9.00e-2$	3.67	$1.16e-1$	3.94	0.016
16	$3.18e-2$	1.94	$1.48e-2$	1.95	0.031	$7.05e-3$	4.07	$7.56e-3$	3.87	0.016
32	$8.29e-3$	2.00	$3.82e-3$	1.99	0.031	$4.20e-4$	4.04	$9.63e-4$	3.72	0.031
64	$2.07e-3$	2.00	$9.63e-4$	2.00	0.078	$2.55e-5$	4.00	$3.91e-5$	3.83	0.109
128	$5.17e-4$	2.00	$2.41e-4$	2.00	0.344	$1.59e-6$	4.00	$2.74e-6$	3.91	0.344
256	$1.29e-4$	2.00	$6.03e-5$	2.01	1.094	$9.93e-8$	4.00	$1.82e-7$	3.96	1.172
512	$3.23e-5$	—	$1.50e-5$	—	3.266	$6.20e-9$	—	$1.17e-8$	—	3.656

A mathematical model can show how the infectious disease with HRSV progresses and what are the outcomes of an epidemic of this virus. Recently, a compartmental model was proposed in [Rosa and Torres (2018)], based on stratifying the population into four health states: susceptible to the infection, denoted by S ; a group of individuals E who have been infected but are not infectious yet, which become infectious at a rate ε ; infected and infectious, denoted by I ; and recovered individuals R . A particular property of HRSV is that immunity after infection is temporary, i.e., the recovered individuals become susceptible again [Weber et al. (2001)], hence, the model is called a SEIRS model. The authors of [Rosa and Torres (2018)] considered that the annual recruitment rate is seasonal due to schools opening/closing periods and proposed the following system of FDEs:

$$\begin{cases} {}_0^C D_t^\alpha S(t) = \lambda(t) - \mu S(t) - \beta(t)S(t)I(t) + \gamma R(t), \\ {}_0^C D_t^\alpha E(t) = \beta(t)S(t)I(t) - \mu E(t) - \varepsilon E(t), \\ {}_0^C D_t^\alpha I(t) = \varepsilon E(t) - \mu I(t) - \nu I(t) \\ {}_0^C D_t^\alpha R(t) = \nu I(t) - \mu R(t) - \gamma R(t), \end{cases} \quad (27)$$

with given initial conditions

$$S(0), E(0), I(0), R(0) \geq 0,$$

where μ denotes the birth rate, which was assumed equal to the mortality rate, γ is the rate of loss of immunity, ν is the rate of loss of infectiousness, β denotes the transmission parameter, which is modeled by the cosine function as $\beta(t) = b_0(1 + b_1 \cos(2\pi t + \Phi))$, in which b_0 is the mean of β and b_1 is the amplitude of the seasonal fluctuation, $\lambda(t) = \mu(1 + c_1 \cos(2\pi t + \Phi))$ is the recruitment rate, which includes newborns and immigrants, with c_1 as the amplitude of the seasonal fluctuation, and where ${}_0^C D_t^\alpha$ denotes the left Caputo derivative of order $\alpha \in (0, 1]$. In the parameters β and λ , the parameter Φ is an angle that is chosen in agreement with real data. Note that by introducing the group E , a latency period is included in the model, which is assumed equal to the time between infection and the first symptoms.

4.2 Numerical results

Based on data obtained from the Florida Department of Health, authors in [Rosa and Torres (2018)] searched the fractional order of differentiation, α , that best fits the data on the reported number of positive tests of HRSV disease, per month, during 35 months, precisely between September 2011 and July 2014 in the state of Florida (excluding North region). They found that with $\alpha = 0.993$ the model fits quite well the data of HRSV disease. Using the values of the parameters μ , ν , γ , ε , b_0 , b_1 , c_1 , and Φ as given in Table 3, borrowed from [Rosa and Torres (2018)], and the initial conditions given in Table 4, we applied our numerical scheme to solve the SEIRS- α model given by (27) with $\alpha = 0.993$ and different values of n . Since World Health Organization goals are usually fixed for five years periods for most diseases, it was assumed that $\tau = 5$. By considering $n = 20, 40, 60, 80$, the numerical results of the state variables $S(t)$, $E(t)$, $I(t)$ and $R(t)$, obtained by the proposed method based on GHFs and MHFs, are reported in Figures 5–8. From these figures, we see that by increasing the value of n , the results are in full agreement with those of [Rosa and Torres (2018)], which in contrast with our approach are obtained by indirect methods.

Table 3 Parameters of the SEIRS- α model borrowed from [Rosa and Torres (2018)].

μ	ν	γ	ε	b_0	b_1	c_1	Φ
0.0113	36	1.8	91	88.25	0.17	0.17	$\frac{\pi}{7}$

Table 4 Initial conditions in terms of percentage of total population.

$S(0)$	$E(0)$	$I(0)$	$R(0)$
0.4081	0.0110	0.0278	0.5531

5 Concluding remarks

We introduced a new numerical approach for solving systems of fractional differential equations (FDEs). In our method,

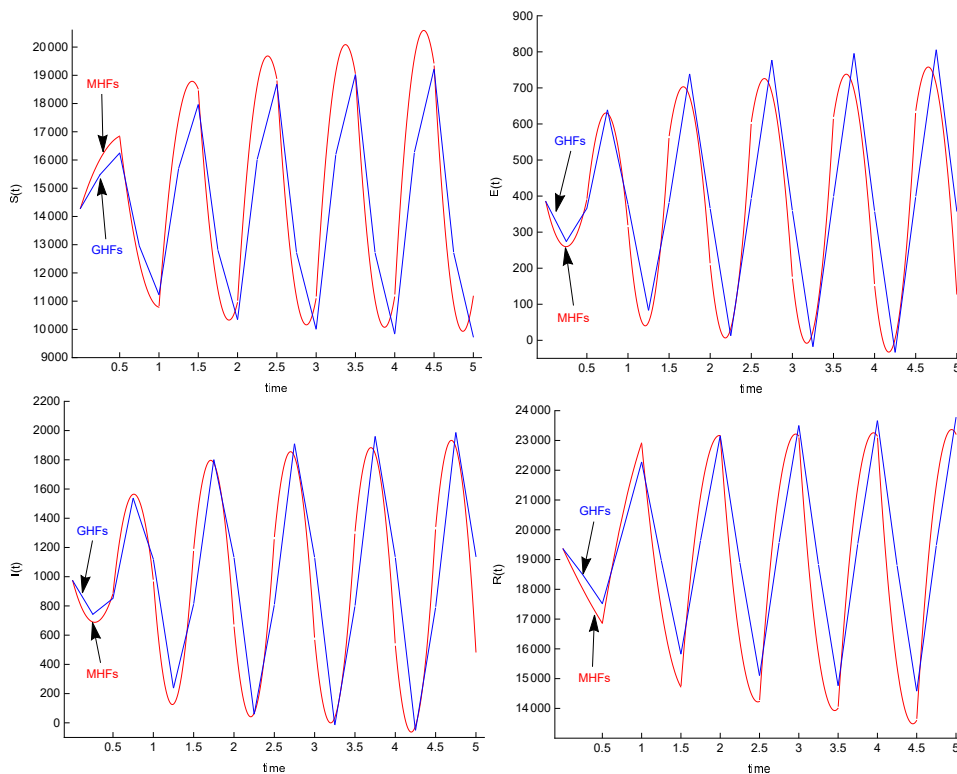


Fig. 5 Numerical results of the state variables of the SEIRS- α model given by (27) based on GHFs and MHFs with $n = 20$, considering $\alpha = 0.993$.

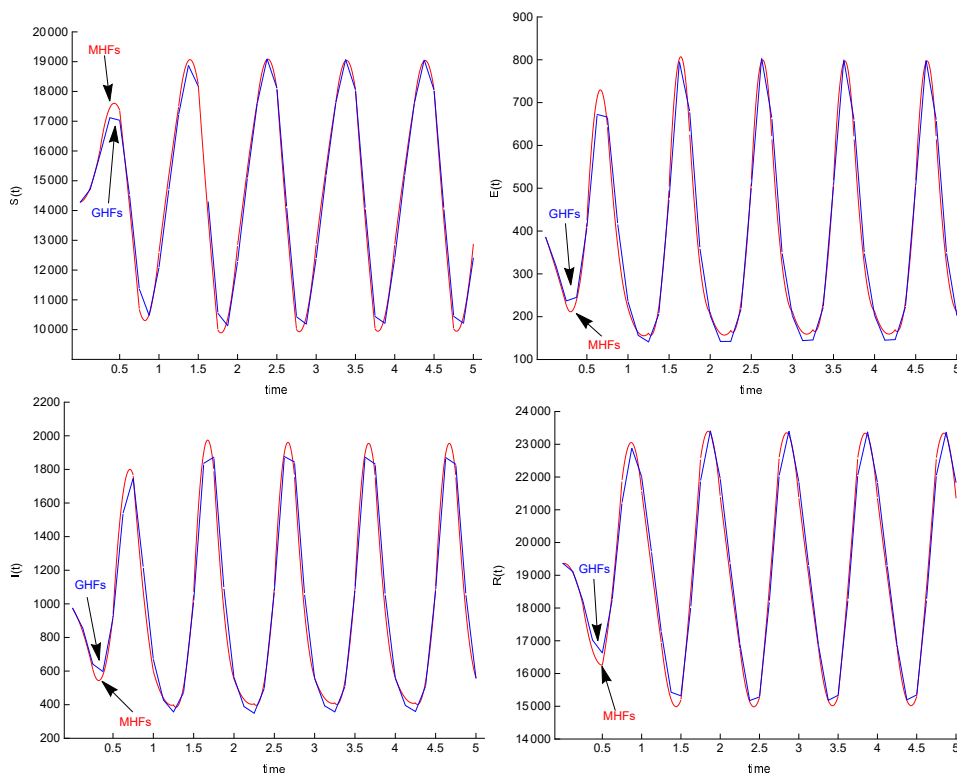


Fig. 6 Numerical results of the state variables of the SEIRS- α model given by (27) based on GHFs and MHFs with $n = 40$, considering $\alpha = 0.993$.

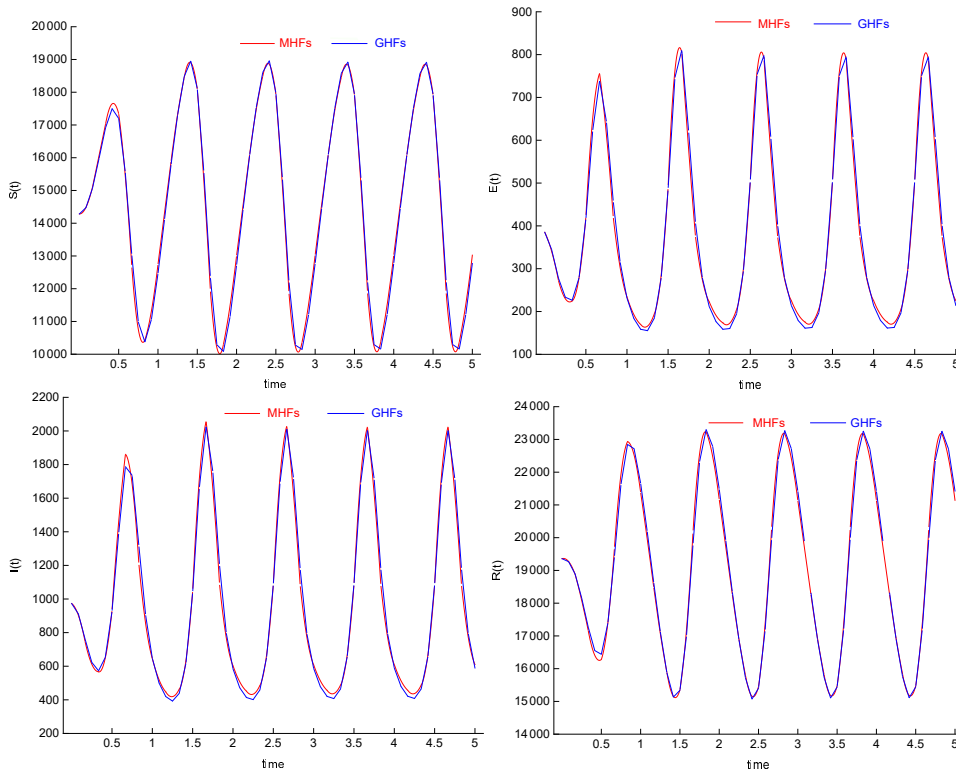


Fig. 7 Numerical results of the state variables of the SEIRS- α model given by (27) based on GHFs and MHFs with $n = 60$, considering $\alpha = 0.993$.

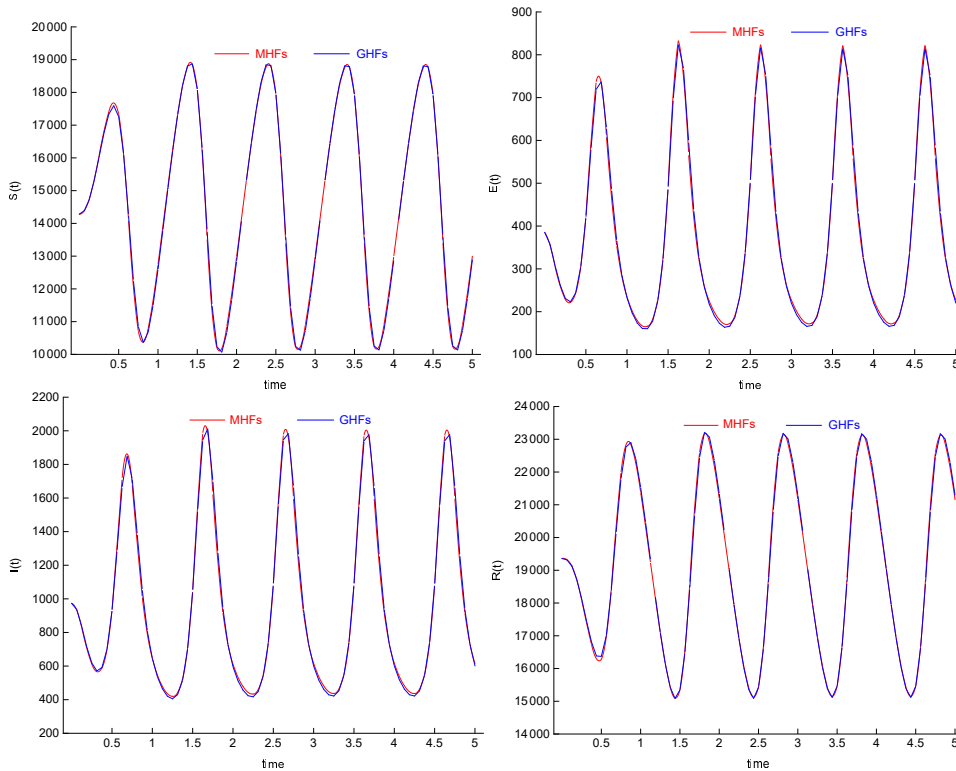


Fig. 8 Numerical results of the state variables of the SEIRS- α model given by (27) based on GHFs and MHFs with $n = 80$, considering $\alpha = 0.993$.

two classes of hat functions, namely generalized hat functions (GHFs) and modified hat functions (MHFs), have been used as the basis functions. In this new scheme, the considered system of FDEs is easily reduced to a system of nonlinear algebraic equations that, according to the computational complexity, needs few computational efforts in both cases of basis functions. By applying the method to two test problems, we see that the numerical results confirm the $O(h^2)$ accuracy order of the GHFs and the $O(h^3)$ accuracy order of the the MHFs. Finally, the method is successfully applied to a mathematical model in epidemiology given by a system of FDEs with application to human respiratory syncytial virus infection.

Acknowledgements Torres was supported by the Portuguese national funding agency for science, research and technology (FCT), within project UID/MAT/04106/2019 (CIDMA). The authors are grateful to two anonymous referees for several positive and constructive comments, which helped them to improve the manuscript.

Compliance with ethical standards

Conflict of interest. The authors declare that they have no conflict of interest.

Ethical approval. This article does not contain any studies with human participants or animals performed by any of the authors.

References

- Agarwal et al. (2015). Agarwal P, Choi J, Paris RB (2015) Extended Riemann–Liouville fractional derivative operator and its applications. *J Nonlinear Sci Appl* 8:451–466, DOI: 10.22436/jnsa.008.05.01
- Ali et al. (2019). Ali MS, Shamsi M, Khosravian-Arab H, Torres DFM, Bozorgnia F (2019) A space-time pseudospectral discretization method for solving diffusion optimal control problems with two-sided fractional derivatives. *J Vib Control* 25(5):1080–1095, DOI: 10.1177/1077546318811194 arXiv:1810.05876
- Almeida et al. (2019). Almeida R, Tavares D, Torres DFM (2019) The variable-order fractional calculus of variations. *SpringerBriefs in Applied Sciences and Technology*, Springer, Cham, DOI: 10.1007/978-3-319-94006-9 arXiv:1805.00720
- Atkinson et al. (2009). Atkinson KE, Han W, Stewart D (2009) Numerical solution of ordinary differential equations. John Wiley & Sons, DOI: 10.1002/9781118164495
- Babolian and Mordad (2011). Babolian E, Mordad M (2011) A numerical method for solving systems of linear and nonlinear integral equations of the second kind by hat basis functions. *Comput Math Appl* 62(1):187–198, DOI: 10.1016/j.camwa.2011.04.066
- Baleanu et al. (2012). Baleanu D, Diethelm K, Scalas E, Trujillo JJ (2012) Fractional calculus, Series on Complexity, Nonlinearity and Chaos, vol 3. World Scientific Publishing Co. Pte. Ltd., Hackensack, NJ, DOI: 10.1142/9789814355216
- El-Sayed and Agarwal (2019). El-Sayed AA, Agarwal P (2019) Numerical solution of multiterm variable-order fractional differential equations via shifted Legendre polynomials. *Math Method Appl Sci* 42(11):3978–3991, DOI: 10.1002/mma.5627
- Heydari et al. (2014). Heydari MH, Hooshmandasl MR, Maalek Ghaini FM, Cattani C (2014) A computational method for solving stochastic Itô–Volterra integral equations based on stochastic operational matrix for generalized hat basis functions. *J Comput Phys* 270:402–415, DOI: 10.1016/j.jcp.2014.03.064
- Jafarian et al. (2018). Jafarian A, Measoomy Nia S, Khalili Golmankhaneh A, Baleanu D (2018) On artificial neural networks approach with new cost functions. *Appl Math Comput* 339:546–555, DOI: 10.1016/j.amc.2018.07.053
- Jafarian et al. (2017). Jafarian A, Rostami F, Golmankhaneh AK, Baleanu D (2017) Using ANNs approach for solving fractional order Volterra integro-differential equations. *Int J Comput Sys* 10(1):470–480, DOI: 10.2991/ijcis.2017.10.1.32
- Malinowska et al. (2015). Malinowska AB, Odziejewicz T, Torres DFM (2015) Advanced methods in the fractional calculus of variations. *SpringerBriefs in Applied Sciences and Technology*, Springer, Cham, DOI: 10.1007/978-3-319-14756-7
- Mirzaee and Hadadiyan (2015). Mirzaee F, Hadadiyan E (2015) Numerical solution of linear Fredholm integral equations via two-dimensional modification of hat functions. *Appl Math Comput* 250:805–816, DOI: 10.1016/j.amc.2014.10.128
- Mirzaee and Hadadiyan (2016a). Mirzaee F, Hadadiyan E (2016a) Approximation solution of nonlinear Stratonovich Volterra integral equations by applying modification of hat functions. *J Comput Appl Math* 302:272–284, DOI: 10.1016/j.cam.2016.02.015
- Mirzaee and Hadadiyan (2016b). Mirzaee F, Hadadiyan E (2016b) Numerical solution of Volterra–Fredholm integral equations via modification of hat functions. *Appl Math Comput* 280:110–123, DOI: 10.1016/j.amc.2016.01.038
- Morales-Delgado et al. (2019). Morales-Delgado VF, Gómez-Aguilar JF, Saad KM, Khan MA, Agarwal P (2019) Analytic solution for oxygen diffusion from capillary to tissues involving external force effects: A fractional calculus approach. *Physica A* 523:48–65, DOI: 10.1016/j.physa.2019.02.018
- Nemati and Lima (2018). Nemati S, Lima PM (2018) Numerical solution of nonlinear fractional integro-differential equations with weakly singular kernels via a modification of hat functions. *Appl Math Comput* 327:79–92, DOI: 10.1016/j.amc.2018.01.030
- Nemati et al. (2018). Nemati S, Lima P, Sedaghat S (2018) An effective numerical method for solving fractional pantograph differential equations using modification of hat functions. *Appl Numer Math* 131:174–189, DOI: 10.1016/j.apnum.2018.05.005
- Nemati et al. (2019). Nemati S, Lima PM, Torres DFM (2019) A numerical approach for solving fractional optimal control problems using modified hat functions. *Commun Nonlinear Sci Numer Simulat* 78:104849, DOI: 10.1016/j.cnsns.2019.104849 arXiv:1905.06839
- Nigmatullin and Agarwal (2019). Nigmatullin RR, Agarwal P (2019) Direct evaluation of the desired correlations: Verification on real data. *Physica A* 534:121558, DOI: 10.1016/j.physa.2019.121558
- Podlubny (1999). Podlubny I (1999) Fractional differential equations, Mathematics in Science and Engineering, vol 198. Academic Press, Inc., San Diego, CA
- Rekhviashvili et al. (2019). Rekhviashvili S, Pskhu A, Agarwal P, Jain S (2019) Application of the fractional oscillator model to describe damped vibrations. *Turk J Phys* 43:236–242, DOI: 10.3906/fiz-1811-16
- Rosa and Torres (2018). Rosa S, Torres DFM (2018) Optimal control of a fractional order epidemic model with application to human respiratory syncytial virus infection. *Chaos Solitons Fractals* 117:142–149, DOI: 10.1016/j.chaos.2018.10.021 arXiv:1810.06900
- Tariboon et al. (2015). Tariboon J, Ntouyas SK, Agarwal P (2015) New concepts of fractional quantum calculus and applications to impulsive fractional q-difference equations. *Adv Differ Equ* 2015:18, DOI: 10.1186/s13662-014-0348-8

- Tripathi et al. (2013). Tripathi MP, Baranwal VK, Pandey RK, Singh OP (2013) A new numerical algorithm to solve fractional differential equations based on operational matrix of generalized hat functions. *Commun Nonlinear Sci Numer Simul* 18(6):1327–1340, doi: 10.1016/j.cnsns.2012.10.014
- Weber et al. (2001). Weber A, Weber M, Milligan P (2001) Modeling epidemics caused by respiratory syncytial virus (RSV). *Math Biosci* 172(2):95–113, doi: 10.1016/S0025-5564(01)00066-9